

Experimental Study on Dynamic Mechanical Properties of Projectile 155 mm ERFB BT Material

Rajesh B. Ohol^{#,*}, Tekram N. Parshuramkar[§], B.A. Parate¹ and Dineshsingh G. Thakur[#]

[#]DRDO-Defence Institute of Advanced Technology, Deemed University, Pune - 411 025, India

[§]Ordnance Factory, Ambajhari, Nagpur - 440 021, India

¹DRDO-Armament Research and Development Establishment, Pune - 411 021, India

*E-mail: ohol_rajesh@yahoo.com

ABSTRACT

Artillery projectile 155mm high explosive (HE) extended range full bore boat tail (ERFB BT) and its components experience a high pressure loading of the propellant during gun launch. Mechanical properties of an engineering material are measured using quasi-static tensile test at room temperature. The materials of the projectile and its components are expected to survive time dependent propellant pressure loading inside the gun, which lasts for few microseconds. To investigate dynamic mechanical properties of the projectile and its components at medium strain rates and elevated temperature, the experimental analysis is undertaken. This research paper aims to examine the effect of medium strain rates and elevated temperatures on flow properties of the materials used in the projectile. The uniaxial tensile tests at the medium strain rates between 0.01 s^{-1} to 1 s^{-1} and at elevated temperatures ranging between 150°C to 500°C are performed separately. The Considère criterion was applied to evaluate strain hardening exponent of the materials. Values of strain hardening exponents of shell body and boat tail materials are less than that of driving band material. Strain rate sensitivity of the materials is observed to be very low, thus indicating a good resistance to plastic deformation. The yield strength and true yield strength of the materials fall with increase in temperature.

Keywords: Quasi-static; Dynamic mechanical properties; Medium strain rate; Strain hardening exponent; Considère criterion

1. INTRODUCTION

The materials used in artillery projectile 155 mm HE ERFB boat tail are subjected to a high acceleration and must possess a high strength to survive the firing stresses. The structural integrity of the projectile and its components is important in internal ballistics. The mechanical properties of materials under intense shock loading differ from the properties observed in the static loading conditions. Quasi-static tensile tests provide the basic design information about materials strength; do not describe the correct mechanical behavior of material experiencing the intense shock loading occurring within a short time. Dynamic tension tests have the range of strain rates between 10^{-1} to 10^2 s^{-1} . As a consequence, study of the flow properties of projectile material is necessary to predict the mechanical response of the projectile and its components subjected to dynamic loading resulting from the propellant during the gun launch conditions.

In recent past, several researchers have studied the effect of elevated temperatures on mechanical properties of non-ferrous and ferrous materials, at high strain rates. Li¹, *et al.* reported a method to determine strain hardening exponent and strength coefficient of 86 kinds of steels. The method developed equations relating the strain hardening exponent and strength

coefficient. Gray III² reported tensile testing machines with servo-hydraulic valves of high capacity, data acquisition and high-speed instruments to measure strain rate up to 200 s^{-1} . A technique of Split Hopkinson Pressure Bar (SHPB) can be used to determine dynamic stress-strain at high strain rate up to $2 \times 10^4 \text{ s}^{-1}$ in compression, and moderately lower in tension and torsion. The characterization of metals using SHPB with a high speed recording was carried out by Nobel³, *et al.* The study investigated the rise in adiabatic temperature during the high rate deformation. Li⁴, *et al.* investigated full-range strain hardening behaviour of the steels. The study presented the formula based on Ramberg-Osgood models that can describe the full range strain hardening of steels.

Shui-sheng⁵, *et al.* performed experiment to consider effect of medium strain rate range on the dynamic strength of metals, brittle materials and polymers. The study showed that the dynamic strength of these materials is sensitive to medium strain range. A dual-phase microstructure of a high specific strength steel (HSSS) was studied by Wang⁶, *et al.*, considering strain rate effect with tensile behaviour. The tensile toughness, the ultimate strength, and the yield strength increase as strain rate increases. Zhang⁷, *et al.* analyzed the study between strain rate and flow stress for TC18 titanium alloy subjected to different impact loads, different temperatures and different strain rates. The study concluded that the yield strength and flow

stress increase slowly with the increase of the strain rate, and the strain value corresponding to the yield strength is reduced, and the flow stress decreases with the increase of experimental temperature. Runda⁸, *et al.* conducted Micro Tensile Tests to estimate dynamic mechanical properties of austenite steel sheets. At room temperature, the tensile tests were performed with various strain rates varying from 0.001 s^{-1} to 10 s^{-1} . The study showed that the increase of strain rate results into a decrease in ductility. Clifton⁹ investigated the high strain rate response of polycrystalline metals, and it was observed that metals exhibit a strong increase in flow stress for strain rates of 10^5 s^{-1} and higher. Meyers¹⁰, *et al.* developed the constitutive descriptions of mechanical behaviour of metals to investigate the instability, slip-twinning transition, grain size effects and shock compression. The steel grade¹¹⁻¹² plays a key role in deciding an effect of tensile steel properties on the loading rates. The sensitivity is dependent upon the strength level. The effect of temperature up to 437 K on the flow properties of materials was studied for different metals. Simon¹³, *et al.* investigated the sensitivities of high strength steel experimentally, and the comparisons between five different constitutive models predictions and the experimental results were made. As regards to Cu alloy, the tensile properties of Cu-Cr-Zr-Ti alloy¹⁴ in annealed condition were studied with different strain rates varying between 10^{-4} s^{-1} to 10^{-1} s^{-1} at different temperatures 300 °C, 450 °C, 600 °C and 700 °C. The study concluded that the yield strength and ultimate tensile strength vary with the strain rate and temperature.

The mechanical characterization of aluminum alloy AA 7449-T7651 was carried out at a high strain rates from room temperature up to elevated temperatures¹⁵. The experimental data was used to derive the constants of the material models, Cowpers Symonds and Johnson- Cook. The flow stress and maximum stress are affected by temperature as well as strain rate. Zhang¹⁶, *et al.* studied an applicability of the theoretical formulas of ten alloys; the study concluded that the traditional formulas relating strength coefficient, fracture strength, strain hardening exponent and fracture ductility can be used only under certain conditions. Altan and Boulger¹⁷ used flow stress data of metals in the simple formulas to predict the pressure required for metal forming. Dieter¹⁸, *et al.* explained the effects of testing conditions on flow properties of metals. Poehlandt¹⁹ laid down the procedure for evaluation of stress-strain curves by tensile tests.

Rakvåg²⁰, *et al.* studied the fracture modes and various deformations that may occur in the steel projectiles during an impact by carrying out Taylor bar impact tests followed by metallurgical investigation of fracture projectile surfaces. The study concluded that the mode of fracture of ductile projectiles is the combination of tensile splitting and spiral shear. Singh²¹, *et al.* carried out the study to estimate the dynamic yield strength of mild steel, which is impacted by the steel balls having velocity between 1900-5200m/s. The study showed that dynamic strength of target material i.e. mild steel is dependent on impact velocity and strain rate wherein the material deformation takes place. Yin²², *et al.* carried out a comprehensive multi physics analysis of the launch process of precision guided projectiles taking into account the coupled

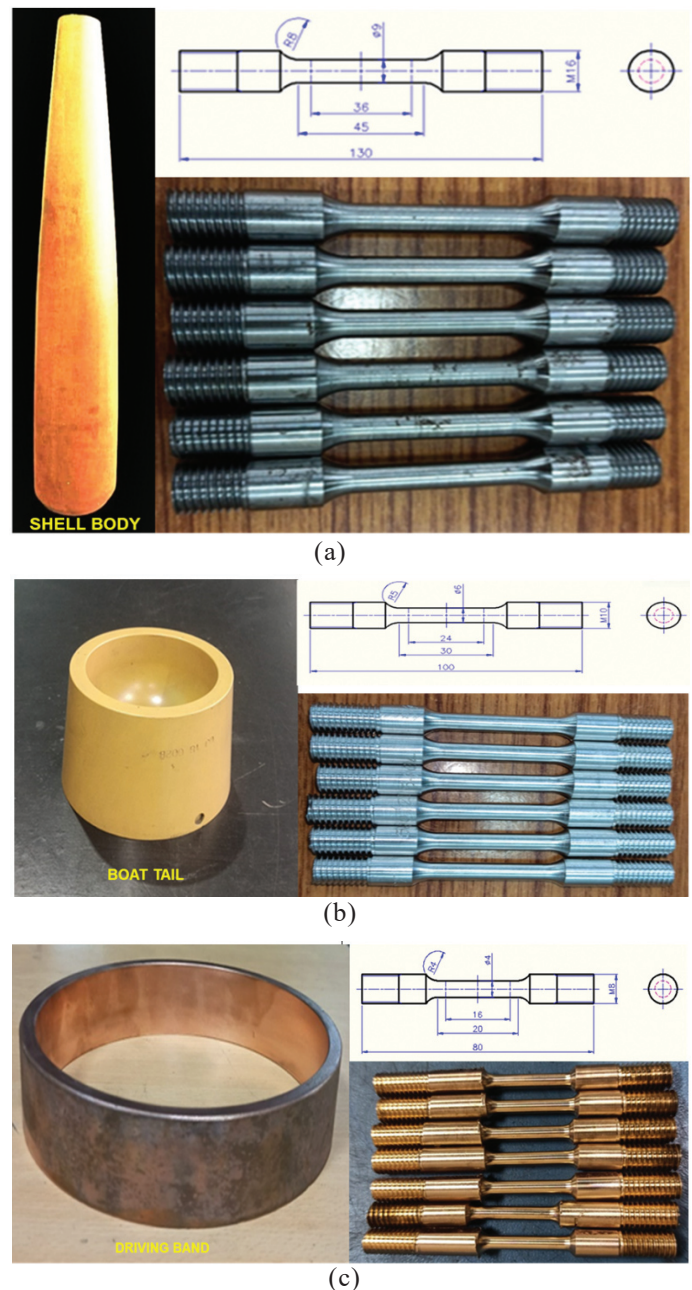


Figure 1. Projectile components: (a) Shell body - AISI 9260 & tensile test specimens; (b) Boat tail - Al alloy 7075 T6 and tensile test specimens; (c) Driving band – CuZn10 and tensile test specimens.

effects between propellant, projectile, confined volume and free space. It was concluded that the complex phenomena of launch process are characterized by high oscillatory pressure profiles and projectile springback. Verberne²³, *et al.* examined the solid-solid interaction involving the projectile and the barrel. The dynamics of the launch process of the projectile inside the gun barrel was studied by conducting finite element simulation. The work revealed the effect of the frictional forces between projectile and barrel on the projectile's acceleration response at muzzle exit. A 3D dynamic analysis of projectile 155 mm ERFB BT during gun launch conditions²⁴ using finite element code, ABAQUS/Explicit was carried out to investigate the plastic deformation of shell body and boat applying true stress-strain curves of the materials. The study affirmed the

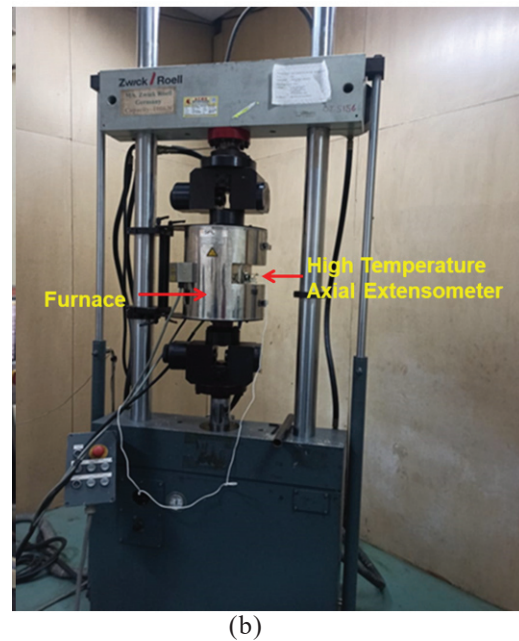


Figure 2. Experimental setup: (a) Tensile specimen under uniaxial tests at medium rates, and (b) Tensile specimen under uniaxial testing at elevated temperature.

structural integrity of the projectile inside the gun barrel at maximum chamber pressure.

Furthermore, many studies related to mechanical behaviour and ballistic properties of armor materials were reported by the researchers. Thus, the published literature work is mainly limited to the impact analysis involving armour materials struck by armour piercing projectiles. The estimation methods reported by the researchers can only present approximate values of strain hardening exponent of metals, and cannot replace experimental testing. To obtain reliable tensile properties, the experimental testing is essential for the accurate design analysis.

The current paper presents a comprehensive experimental study covering uniaxial tensile tests at various medium strain rates and elevated temperatures of AISI 9260, Al Alloy 7075 T6 and Cu-Zn10 alloy materials, which are used for shell body, boat tail and driving band respectively as the projectile main components. The study aims to elucidate experimentally the strain hardening behavior and flow properties of materials of the projectile from the point of view of plastic deformation. Uniaxial tensile tests are conducted at medium strain rates and elevated temperatures separately. Flow properties of these materials are investigated experimentally. An effect of medium strain rate on material strength of shell body, boat tail and driving band is analyzed. The strain hardening behavior of the materials due to plastic deformation, and the variations in materials true yield strength and true stress with temperature rise are studied.

2. EXPERIMENTAL PROCEDURE AND SETUP

To investigate the quasi-static and dynamic tensile properties experimentally, fourteen specimens each from shell body, boat tail and driving band materials were prepared as per the standard ASTM E8²⁵ for uniaxial tensile tests as depicted in

Fig. 1(a-c). In the first stage of experiments, the uniaxial tensile tests were performed on the specimens at medium strain rates 0.000625 s^{-1} , 0.01 s^{-1} , 0.1 s^{-1} , 0.2 s^{-1} , 0.3 s^{-1} , 0.4 s^{-1} , 0.5 s^{-1} and 1 s^{-1} . Conventional servo-hydraulic or screw driven tensile testing apparatus can measure stress-strain response of materials up to 1 s^{-1} . The servo-hydraulic system Universal Testing Machine (UTM), Model: LFV 250 HH, Capacity: 250 kN, Make: Walter Bai was used to conduct the tests. Figure 2(a) depicts the experimental setup. During the second phase of experiments, the uniaxial tensile tests were performed on the specimens at the temperatures 27°C , 150°C , 200°C , 250°C , 350°C and 500°C as per ASTM E21²⁶ on the servo-hydraulic system UTM, Model: HA-100, Capacity: 100 kN, Make: Zwick Roell as shown in Figure 2 (b). The axial extensometer of Gauge Length: 25.00 mm, Model: 3542-025M-10-ST, Range (Travel): $\pm 10\%$ (2.50 mm), Make: Epsilon Technology Corp, Jackson, WY. USA and the high temperature axial extensometer of Gauge Length: 25 mm, Model: 3448-025M-20, Range (Travel): $\pm 20\%$ ($\pm 5.00 \text{ mm}$), Make: Epsilon Technology Corp, Jackson, WY. USA were employed for carrying out tensile tests.

3. FLOW CURVE EQUATION

3.1 Flow Curves or Power Curves Equation of Metal

Flow curve of the metals²⁷ is expressed by power curve relation as under:

$$\sigma = K \varepsilon^n \quad (1)$$

where K = strength coefficient, ε = true strain, n = strain-hardening exponent and σ = true stress. If the metal obeys Eqn. (1), then the graph of $\log \sigma$ versus $\log \varepsilon$ up to maximum load is a straight line, whose slope is the strain-hardening exponent (n). In this study, for determination of strain hardening exponent, the tensile tests were performed at quasi-static strain rate of 0.000625 s^{-1} . A necking criterion using engineering strain is given as under:

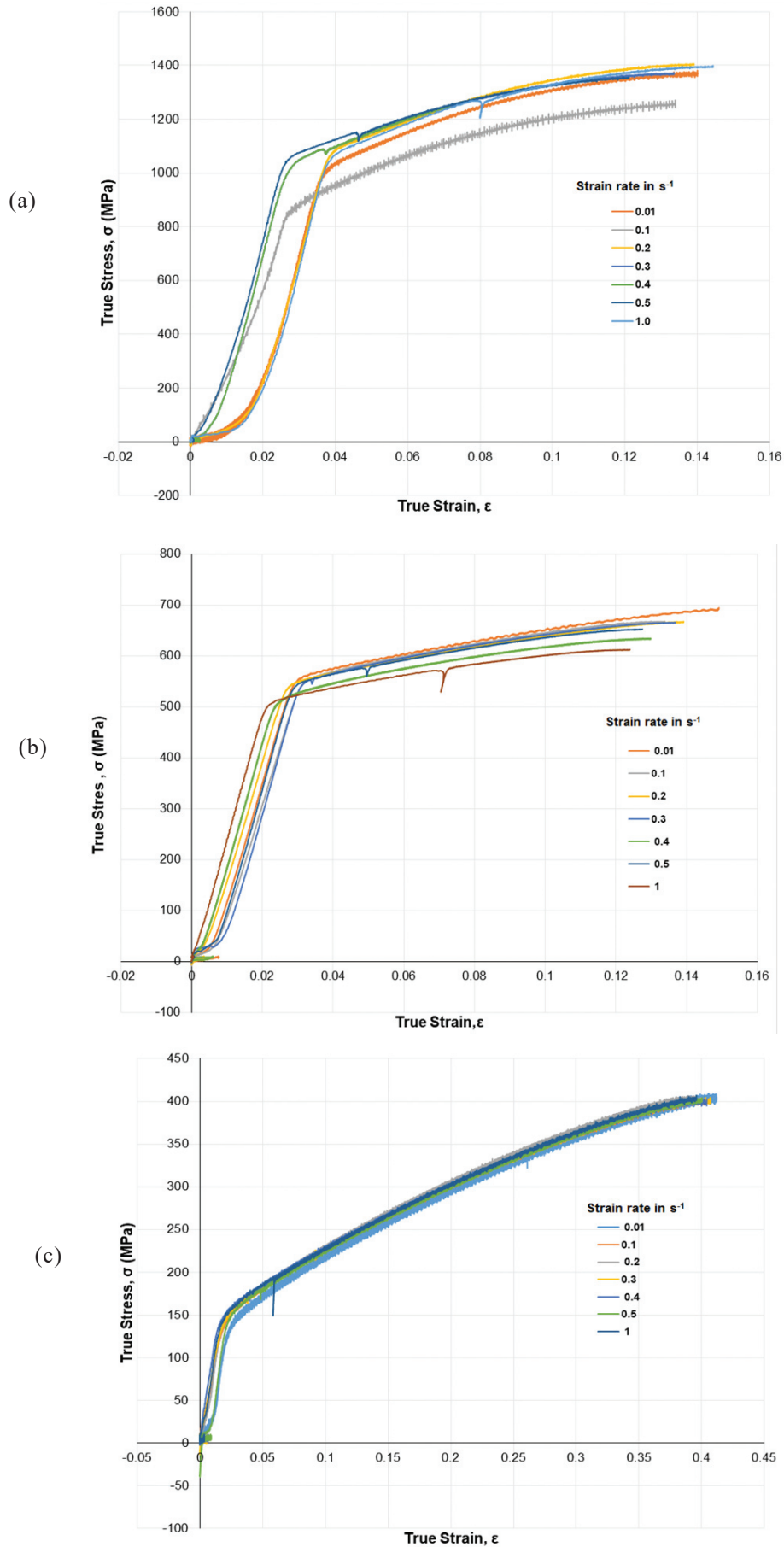


Figure 3. True stress-strain curves at various medium strain rates: (a) AISI 9260, (b) Al alloy 7075 T6, and (c) Cu-Zn10. (these curves are plotted only up to maximum stress point.)

Table 1. Tensile properties at quasi-static and medium strain rate

Material	Tensile properties			
	Quasi-static strain rate 0.000625 s ⁻¹		Medium strain rate 1 s ⁻¹	
	True yield strength (MPa)	True tensile strength (MPa)	True yield strength (MPa)	True tensile strength (MPa)
Alloy steel AISI 9260	900	1300	1030	1380
Al alloy 7075 T6	440	585	550	690
Cu-Zn10	95	350	140	380

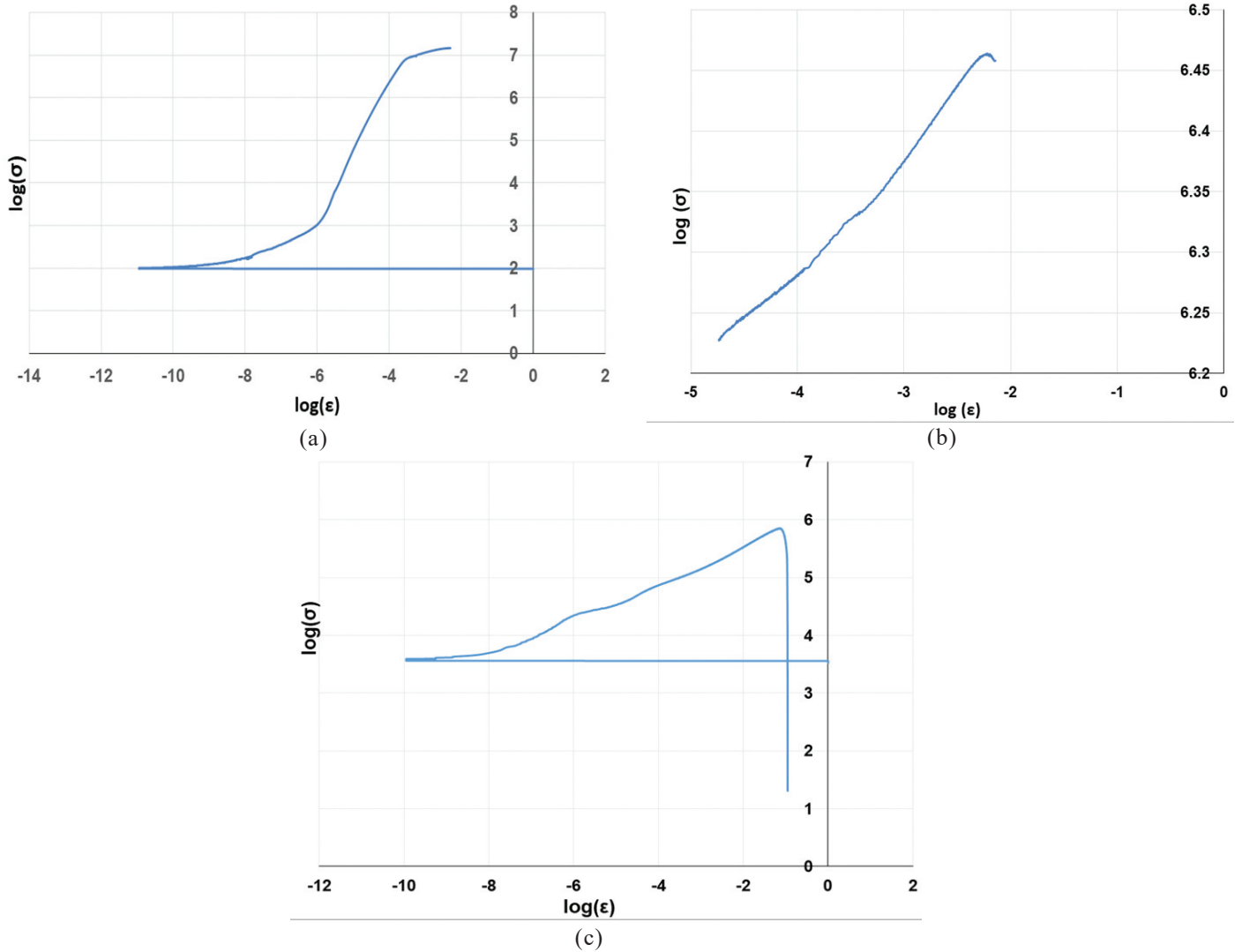


Figure 4. Log-log plot of the true stress-strain curves: and (a) AISI 9260, (b) Al alloy 7075 T6, (c) Cu-Zn10.

$$\frac{d\sigma}{de} = \frac{\sigma}{1+e} \quad (2)$$

where, e = engineering strain and σ = true stress. Following relation between the strain hardening exponent and the true uniform strain (ϵ_u) is treated as the Considère criterion:-

$$\epsilon_u = n \quad (3)$$

True uniform strain (ϵ_u) is defined as the true strain up to maximum load. Eqn. (3) is not dependent on the power law behaviour²⁸.

3.2 Influence of Strain Rate on Flow Properties of Materials

Strain rate affects true stress-strain graph. Flow stress increases as strain rate increases. Each type of mechanical test has a range of strain rate. It is known as the rate of change of the strain per unit time. Its unit is the reciprocal of second.

$$\dot{\epsilon} = \frac{d\epsilon}{dt} \quad (4)$$

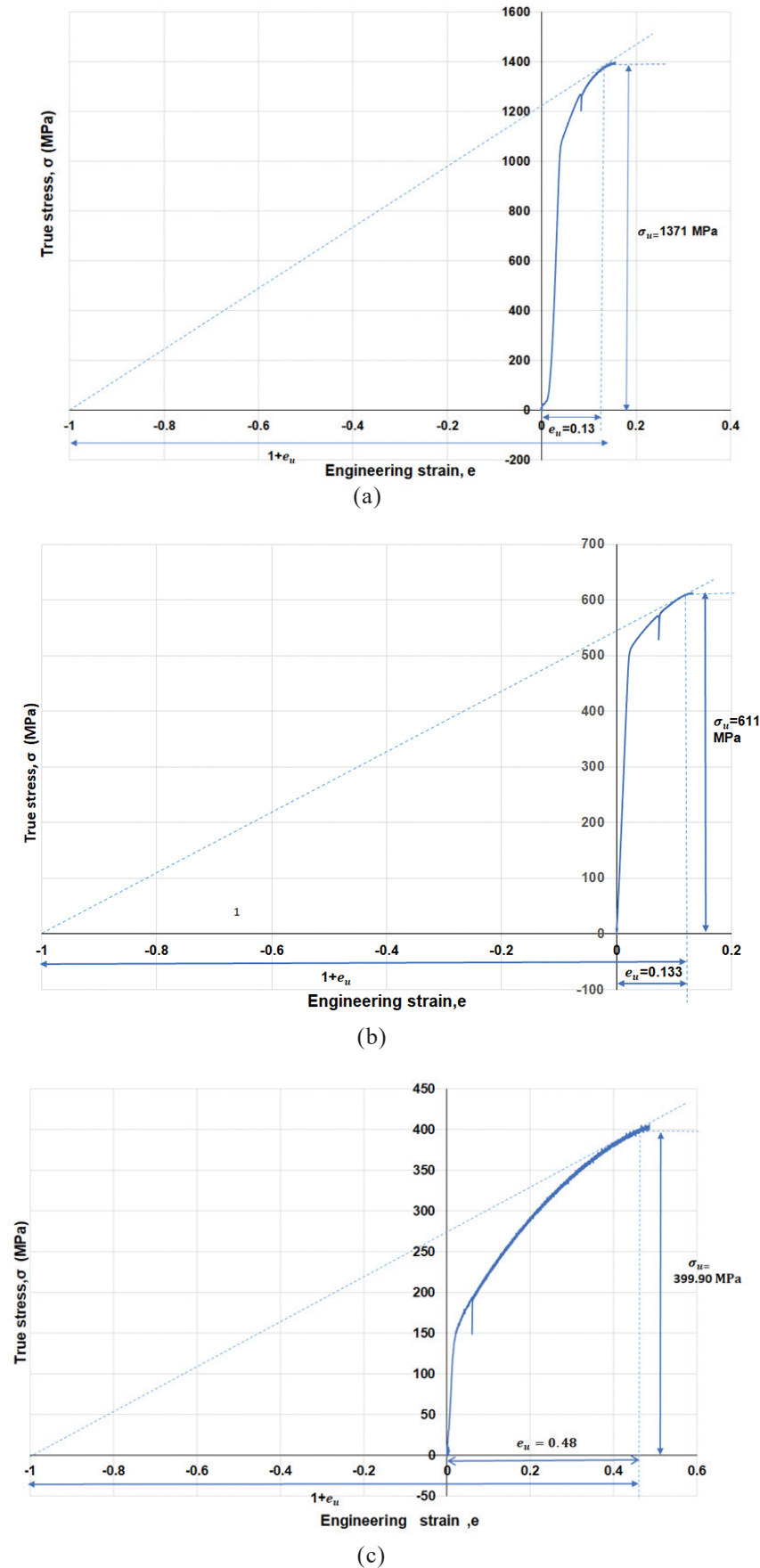


Figure 5. True stress vs. engineering strain curves: (a) AISI 9260, (b) Al alloy 7075 T6, and (c) CuZn10. (These curves are plotted only up to maximum stress point.)

4. DYNAMIC MECHANICAL BEHAVIOR OF PROJECTILE MATERIALS

4.1 True Stress True Strain Curves

To understand the plastic flow of the materials of the projectile, true stress-true strain curves at 0.01s^{-1} , 0.1s^{-1} , 0.2s^{-1} , 0.3s^{-1} , 0.4s^{-1} , 0.5s^{-1} , 1s^{-1} were plotted applying the following Eqns:

$$\varepsilon = \ln(e + 1) \quad (5)$$

where, ε is true strain and e is conventional or engineering strain.

$$\sigma = s(1 + e) \quad (6)$$

where, σ is true stress and s is conventional or engineering stress. The Eqns (5)-(6) are applicable up to maximum load. The true stress-true strain curves of the materials plotted up to maximum stress points are shown in Fig. 3(a-c).

The tensile properties at the quasi-static strain rate 0.000625 s^{-1} and at maximum medium strain rate 1 s^{-1} are obtained from the experiments. The true yield stress and true tensile stress values of the materials are shown in Table 1.

4.2 Strain Hardening Exponent (n) of Projectile Materials

Initially, the log-log profile of the true stress-strain curve of each material is considered to obtain the strain hardening exponent (n). Figures 4 (a-c) show the log-log profiles of the true stress-stress graphs of AISI 9260, Al Alloy 7075 T6 and Cu-Zn10 materials, respectively.

The non-linear relations are observed in the log-log graphs of the materials, which transpire that the materials do not follow Hollomon equation. Samuel²⁹ showed that all materials illustrate the deviation from an ideal Hollomon equation at a low strains. To get value of n , the Considère construction is adopted and a curve of true stress versus engineering strain at strain rate 1 s^{-1} is plotted for each material based on the experimental values. Applying Eqn (3), n is determined from the Considère construction as shown in Fig. 5(a-c). The values of n obtained are given in Table 2.

Table 2. Strain hardening exponent of materials

Material	Engg strain at true tensile strength (ε_u)	True uniform strain $\varepsilon_u = \ln(e_u + 1)$	Strain hardening exponent (n)
AISI 9260	0.13	0.12	0.12
Al alloy 7075 T6	0.13	0.12	0.12
Cu-Zn10	0.48	0.39	0.39

4.3 Strain Rate Sensitivity (m)

Strain rate sensitivity (m) is measured by plotting two true stress-strain curves at different strain rates and comparing the true stress levels at a fixed strain³⁰. The following equation is used:

$$m = \frac{\ln \frac{\sigma_2}{\sigma_1}}{\ln \frac{\dot{\varepsilon}_2}{\dot{\varepsilon}_1}} \quad (7)$$

The values of ε_1 , ε_2 , σ_1 and σ_2 of each material are obtained

from the respective plots as shown in Fig. 6 (a-c). m values of AISI 9260, Al alloy 7075 T6 and Cu-Zn10 materials are given in Table 3.

4.4 Effect of High Temperature on Mechanical Behavior

To study the effect of high temperatures on the mechanical behavior of the materials for shell body, boat tail and driving band, the uniaxial tensile tests at strain rate 0.000625 s^{-1} were performed on the specimens at the temperatures $27\text{ }^\circ\text{C}$, $150\text{ }^\circ\text{C}$, $200\text{ }^\circ\text{C}$, $250\text{ }^\circ\text{C}$, $350\text{ }^\circ\text{C}$ and $500\text{ }^\circ\text{C}$ as per the standard ASTM E21. Figure 7(a) depicts the curve of yield strength vs. temperature. The relation between true yield stress and temperature is shown in Fig. 7(b).

5. RESULTS AND DISCUSSION

The flow behavior of materials of the projectile is depicted in true stress-strain graphs of materials. The true stress-strain graphs of materials were plotted at different strain rates on the basis of experimental data up to true tensile strength point as shown in Fig. 3(a-c). Strain hardening rate of CuZn10 is found to be relatively higher than that of AISI 9260 and Al alloy 7075 T6. The main reason for the high rate of strain hardening of CuZn10 material is due to the fact that CuZn10 is annealed material whereas other two materials are heat treated. For different strain rates, the curves of the true stress-strain reveal that there is not much change in flow stress pattern. Thus, the materials are not very strain rate sensitive.

It is observed from Fig. 4(a-c) that the materials do not follow Hollomon relation. Strain hardening exponents calculated by applying the Considère criterion make clear that the strain hardening exponent of CuZn 10 material is higher than the strain hardening exponents of AISI 9260 and Al alloy 7075 T6 materials. This is possible because the materials have been given different types of heat treatment. The annealed material has exhibited a high strain hardening exponent, which holds good in agreement. It clearly reveals that the high strength materials viz. Alloy steel AISI 9260 and Al alloy 7075 T6 have low strain hardening exponent than CuZn10 having a low strength. The yield strength of the materials drops with increase in temperature. From Figures 7(a-b), it is observed that as temperature increases the yield stress and true yield stress of the materials decrease due to the effect of temperature on deformation of the material. Al alloy 7075 T6 being precipitation hardenable, it is predicted that Al alloy 7075 T6 has exhibited precipitation coarsening between the temperature $200\text{ }^\circ\text{C}$ to $350\text{ }^\circ\text{C}$, thereby showing rapid drop in yield stress and true yield stress. Moreover, during gun launch conditions, the projectile remains inside gun barrel between the temperature $135\text{ }^\circ\text{C}$ to $170\text{ }^\circ\text{C}$ for maximum 50 millise. Hence, the temperature effect on the yield strength of materials is less significant for plastic deformation of the projectile materials.

6. CONCLUSIONS

This manuscript describes about various experiments carried out for the dynamic behavior of shell body material-alloy steel AISI 9260, boat tail material - Al Alloy 7075 and driving band material - CuZn10 by uniaxial tensile tests

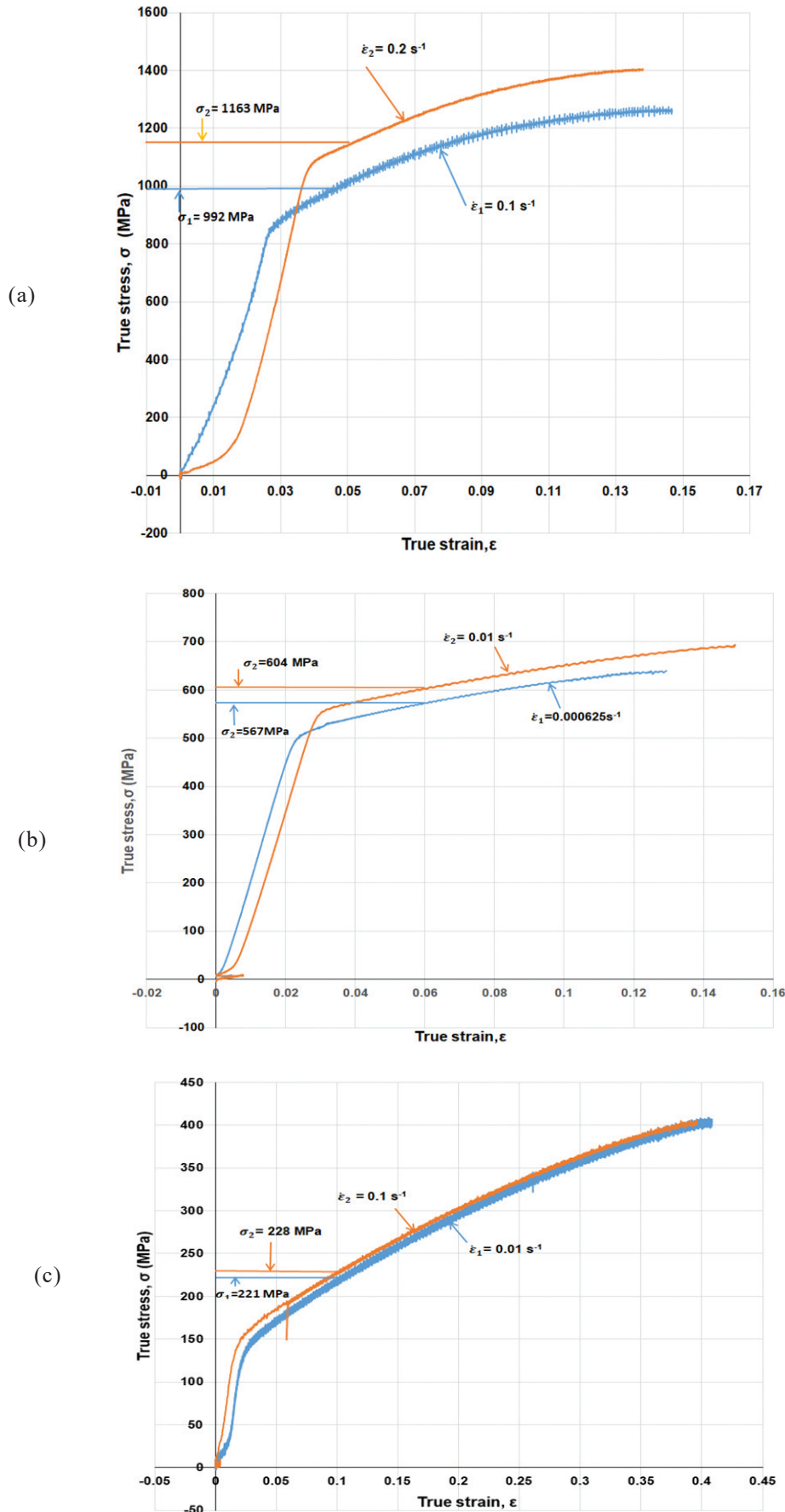


Figure 6. True stress vs. strain curves at two different strain rates: (a) AISI 9260, (b) Al alloy 7075 T6, and (c) Cu-Zn10. (These curves are plotted only up to maximum stress point.)

Table 3. m values of the materials

Material	True strain, ϵ	Strain rate, $\dot{\epsilon}$ (s ⁻¹)		True stress, σ (MPa)		m
		$\dot{\epsilon}_1$	$\dot{\epsilon}_2$	σ_1	σ_2	
AISI 9260	0.05	0.1	0.2	992	1163	0.23
Al alloy 7075 T6	0.06	0.000625	0.01	567	604	0.02
Cu-Zn10	0.1	0.01	0.1	221	228	0.01

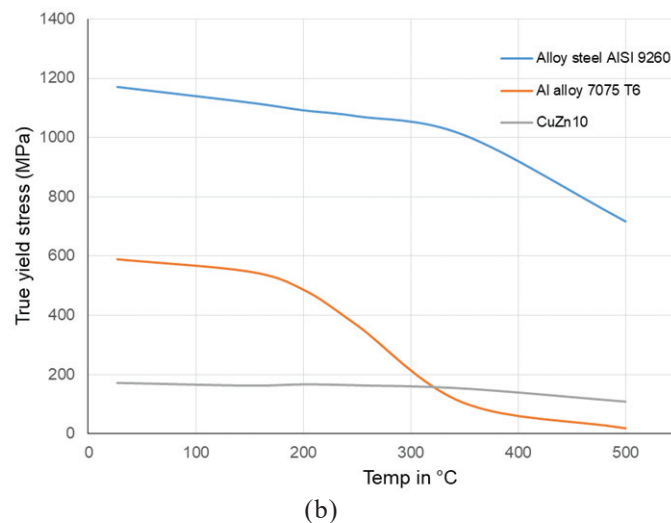
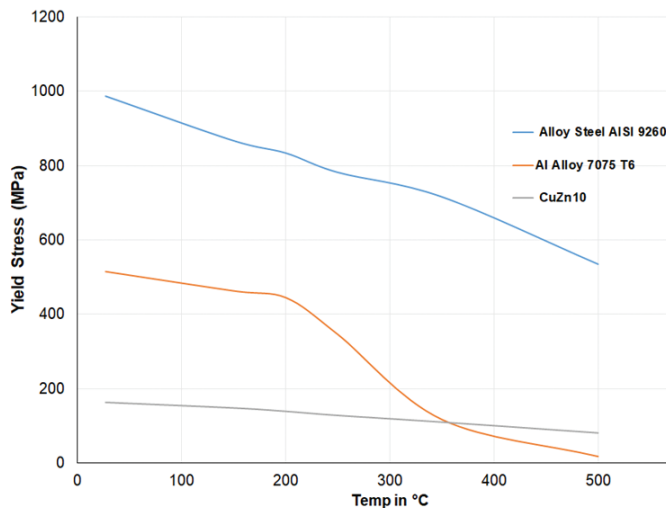


Figure 7. Plots of: (a) Yield stress vs. temperature, (b) True yield stress vs. temperature.

performed at medium strain rates and further characterization at elevated temperatures. Based on these experimental results, following inferences were drawn:

- Alloy steel AISI 9260 being a BCC material has exhibited higher strain rate sensitivity compared to Al alloy and Cu-Zn10 alloy, which are FCC materials
- It is revealed that strain rate influences the flow stresses at lower plastic strains. The flow stress of these materials increases as the strain rate increases
- On comparison between the tensile properties at the quasi-

static strain rate 0.000625 s^{-1} and at maximum medium strain rate 1 s^{-1} , it is identified that the change in the true yield strength is more than the change in the true tensile strength

- The materials of the shell body, boat tail and driving band have exhibited excellent dynamic tensile properties at medium strain rate ranging from 0.01 s^{-1} to 1 s^{-1} . There is no major variation in the strain hardening exponents of the materials, which shows that the shell body and boat tail possess a good resistance to the plastic deformation at medium strain rates. The mechanical behavior of driving band is in good agreement with the norm of design stipulation. It has shown a high rate of strain hardening after yielding
- The yield strength and true yield strength of shell body, boat tail and driving band materials drop with increase in temperature. However, the yield strength and true yield strength of boat tail material i.e. Al alloy 7075 T6 drop rapidly between the temperature 200°C to 350°C . The rapid drop in strength is attributed to precipitation coarsening of the Al alloy 7075 T6 between this temperature range. The drop in the strength of Al alloy 7075 T6 between this temperature range has no any adverse effect on the structural integrity of the projectile because the projectile remains inside the gun barrel having temperature less than 200°C to 350°C during gun launch conditions
- The comprehensive experimental analysis shows that the mechanical properties of the projectile 155 mm ERFB BT materials survive the medium strain rates.

REFERENCES

- Li, J.; Qiu, Y.; Wang, H. & Wang, Z. Estimation of the strength coefficient and strain hardening exponent from monotonic tensile properties of steels. *Int. J. Steel Struct.*, 2019, **19**(6), 1951-1968. doi: 10.1007/s13296-019-00256-w.
- Gray III, G.T. Classic split Hopkinson pressure bar testing. *In Mechanical testing and evaluation. ASM handbook, Vol-8*, ASM International, 2000. pp. 1027-1028.
- Noble, J.; Goldthorpe, B.; Church, P. & Harding, J. The use of the Hopkinson bar to validate constitutive relations at high rates of strain. *J. Mech. Phys. Solid*, 1999, **47**, 1187-1206.
- Li, T.; Zheng, J. & Chen, Z. Description of full range strain hardening behavior of steels. *J. Springer Plus*, 2016, **5**, 1316. doi: 10.1186/s40064-016-2998-3.
- Shui-sheng, Y.; Yu-bin, L. & Yong, C. The strain-rate effect of engineering materials and its unified model. *Lat. Am. J. Solid Struct.*, 2013, **10**, 833-844.
- Wang, W.; Ma, Y.; Yang, M.; Jiang, P.; Yuan, F. & Wu, X. Strain rate effect on tensile behavior for a high specific strength steel: From quasi-static to intermediate strain rates. *J. Met.*, 2018, **8**, 11. doi:10.3390/met8010011.
- Zhang, C.; Mu, A.; Wang, Y. & Zhang, H. Study on dynamic mechanical properties and constitutive model construction of TC18 Titanium alloy. *J. Met.*, 2019, **10**(1),

44.
doi:10.3390/met10010044.
8. Runda, M.; Procházka, R.; Konopík, P.; Džugan, J.; Folgar, H. Investigation of sample-size influence on tensile test results at different strain rates. *In* 1st International Conference on Structural Integrity, Procedia Engineering, Portugal, 2015, **114**, pp. 410 – 415.
doi: 10.1016/j.proeng.2015.08.086.
9. Clifton, R.J. High strain rate behavior of metals. *Appl. Mech. Rev.*, 1990, **43**(5S), S9-S22.
doi:10.1115/1.3120862.
10. Meyers, M.A.; Benson, D.J.; Vöhringer, O.; Kad, B.K.; Xue, Q. & Fu, H.H. Constitutive description of dynamic deformation: Physically-based mechanisms. *Mater. Sci. Eng. A.*, 2002, **322**, 194-216.
- 11 Wallin, K. Fracture toughness of engineering materials – Estimation and application, EMAS Publishing, Birchwood Park, Warrington, UK, 2011.
- 12 Health and safety executive. The behavior of carbon steels at high strain rates and strain limits, BOMEL Limited , UK, Offshore technology report No. OTO 1999 018. October 1999.
13. Simon, P.; Demarty, Y.; Rusinek, A.; & Voyiadjis , G.Z. Material behavior description for a large range of strain rates from low to high temperatures: Application to high strength steel. *J. Met.*, 2018, **8**(10), 795.
doi:10.3390/met8100795.
14. Rao, S.G.; Sharma, V.M.J.; Raman, S.G.S.; Amruth, M.; Narayanan, P.R.; Sharma, S.C. & VenkataKrishnan, P.V. Effects of temperature and strain rate on tensile properties of Cu-Cr-Zr-Ti Alloy. *Mater. Sci. Eng. A.*, 2016, **668**, 97–104.
15. Mylonas, G.I. & Labeas, G.N. Mechanical characterization of aluminum alloy 7449-T7651 at high strain rates and elevated temperatures using split Hopkinson bar testing. *Exp. Tech*, 2014, **38**(2), 26-34.
doi:10.1111/j.1747-1567.2011.00796.x.
16. Zhang, Z.; Li, C.; Sun, Q.; Qiao, Y. & Zhao, W. Formula relating fracture strength and fracture ductility with strength coefficient and strain-hardening exponent, *J. Mater. Eng. Perform.*, 2006, **15**, 618-621.
doi: 10.1361/105994906X124622.
17. Altan, T. & Boulger, F.W. Flow stress of metals and its application in metal forming analyses. *J. Eng. Ind.*, 1973, **95B**(4), 1009–1019.
18. Dieter, G.E. Bulk workability of metals. *In* Handbook of workability and process design, edited by G.E. Dieter, H.A. Kuhn & S.L. Semiatin. ASM International. USA, 2003. pp.22-34.
doi:10.1361/hwpd2003p022
19. Poehlandt, K. Materials testing for the metal forming industry, Springer-Verlag, Berlin, Heidelberg, 1989.
20. Rakvåg, K.G.; Børvik, T.; Westermann, I. & Hopperstad, O.S. An experimental study on the deformation and fracture modes of steel projectiles during impact. *Mater. Des.*, 2013, **51**, 242-256.
21. Singh, M.; Sood, D.; Gupta, R.K.; Kumar, R.; Gautam, P.C.; Sewak, B.; Sharma, A.C. & Mathew, T. Dynamic yield strength of mild steel under impact loading. *Def. Sci. J.*, 2008, **58**(2), 275-284.
22. Yin, X.W.; Verberne, P. & Meguid, S.A. Multiphysics modeling of the coupled behavior of precision-guided projectiles subjected to intense shock loads. *Int. J. Mech. Mater. Des.*, 2014, **10**, 439-450.
doi: 10.1007/s10999-014-9255-0.
23. Verberne, P. & Meguid, S.A. Dynamics of precision guided projectile launch: Solid-solid interaction. *Int. J. Struct. Stab. Dyn.*, 2020, **20**(14), 2043001.
doi:10.1142/S0219455420430014.
24. Ohol, R.B.; Parate, B.A. & Thakur, D.G. An investigation of plastic deformation of high explosive projectile 155 mm during gun launch conditions using finite element method. *Def. Sci. J.*, 2022, **72**(6), 793-800.
doi:10.14429/dsj.72.18197.
25. Standard test methods for tension testing of metallic materials. ASTM E8/E8M-16a, ASTM International, 100 Barr Harbor Drive, P.O. Box C700, West Conshohocken, PA 19428-2959, USA, 2016.
26. American Society for testing and materials. Standard test methods for elevated temperature tension tests of metallic materials. ASTM E21-09, ASTM International, 100 Barr Harbor Drive, P.O. Box C700, West Conshohocken, PA 19428-2959, USA, 2009.
27. Dieter, G.E. Mechanical metallurgy, Ed.3. McGraw Hill Book Company Ltd., UK, 1988. pp.287-290.
28. Geil, G.W. & Carwile, N.L. *J. Res. Natl. Bur. Stand.*, 1950, **45**, 129.
29. Samuel, K.G. Limitations of Hollomon and Ludwigson stress-strain relations in assessing the strain hardening parameters. *J. Phys. D: Appl Phys.*, 2006, **39**, 203-212.
doi:10.1088/0022-3727/39/1/030.
30. Hosford, W.F. & Caddell, R.M. Metal forming: Mechanics and metallurgy, Ed. 3. Combridge University Press, New York, 2007. 54p.

ACKNOWLEDGMENT

Authors are thankful to the Vice Chancellor, DIAT, Deemed University, Pune for allowing this research study at DIAT (DU), Pune. Authors wish to express their gratitude to Director, ARDE, Pune for the technical support. Authors would like to thank the General Manager, Ordnance Factory, Ambajhari, Nagpur for providing the experimental facilities for this research work.

CONTRIBUTORS

Mr Rajesh B. Ohol obtained his M.Tech in Armament and Combat Vehicles from DRDO-DIAT (Deemed University), Pune. He has been working as Assistant Engineer (Quality Assurance) in Directorate General of Quality Assurance, Ministry of Defence, Government of India. His areas of research include: Armament engineering and defect investigation of ammunitions. In this paper, he did the literature survey, performed the experiments, analytical analysis and interpretation of results and prepared the manuscript.

Mr Tekram N. Parshuramkar obtained his MTech. in Armament and Combat Vehicles from DRDO-DIAT (Deemed University), Pune. He is working as Junior Works Manager in Ordnance Factory, Ambajhari, Nagpur. He is involved in manufacturing of empty bodies of Projectile 155 mm, 125 mm and 130 mm calibres. He has gained vast experience in the areas related to cold and hot working of ferrous and non-ferrous metals, advanced manufacturing processes and quality control of engineering precision components. In this study, he prepared the specimen for uniaxial tensile tests, analyzed experimental results and arranged the data for the manuscript.

Dr B.A. Parate obtained his PhD in Mechanical Engg. from DRDO-DIAT (Deemed University), Pune and working as Scientist 'F', Joint Director at DRDO-ARDE, Pune. In this paper, he guided the author and reviewed the manuscript.

Dr Dineshsingh G. Thakur obtained his PhD from IIT, Madras. His research domains are CAD/CAM /Robotics, manufacturing consideration in design, high-speed machining/green machining of aerospace materials, precision robotic welding of aerospace materials, micro-manufacturing/micromachining of 'difficult to cut materials'. Presently, he is a Head of Department of Mechanical Engineering in DRDO-DIAT, (Deemed University), Pune (India). In the present work, he guided the author, reviewed and formatted the manuscript.